Purification, ultrastructure, and chemical analysis of Alzheimer disease amyloid plaque core protein

(neuritic plaque/paired helical filaments/neurofibrillary tangles/fluorescence-activated cell sorting/lipofuscin)

ALEX ROHER*†, DAVID WOLFE‡, MARGARITA PALUTKE‡, AND DEBRA KUKURUGA‡

Departments of *Anatomy and Cell Biology and ‡Pathology, Wayne State University School of Medicine, Detroit, MI 48201

ABSTRACT   Isolation of Alzheimer disease amyloid plaque core protein (APCP) was carried out by repetitive NaDodSO₄/EDTA/sucrose extractions and by Ficoll-400 density-gradient centrifugations. The enriched APCP–Ficoll interface was labeled with the fluorochrome thioflavin T and separated from the contaminating lipofuscin by fluorescence-activated cell sorting. Electron microscopy demonstrated that APCP is made of two different kinds of filaments measuring 5.5–6 nm and 10–12 nm, respectively, and of variable length. Purified APCP and lipofuscin were chemically modified by performic acid oxidation. The amino acid composition of APCP revealed a high content of glycine and valine (30%) and 1% cysteine. By contrast, the protein moiety of the copurified lipofuscin contained 16% cysteine. The amino acid composition of APCP did not resemble that of any known protein.

Alzheimer disease is a dementia characterized by loss of memory, perception, orientation, reasoning, and judgement, by a progressive and protracted course, which eventually terminates the intellectual functions and life of the individual (1–3). Because of the chronic evolution of this disease, the emotional, physical, and economic stresses imposed upon the family of the victim are overwhelming. In countries such as the United States and Great Britain, this syndrome has reached catastrophic epidemiologic proportions, since it afflicts 5% of the population over 65 years of age and as much as 20% of those over 80 years of age (1–4). These numbers will undoubtedly increase as the result of longer life expectancy and of demographic changes. In the United States alone, Alzheimer disease claims ≈120,000 lives per year, making it the most common cause of death after heart disease, cancer, and stroke.

Two main histopathological changes are characteristic of Alzheimer disease. Neurofibrillary tangles (5, 6) are localized in the neurons of the cerebral cortex, hippocampus, amygdaloid complex, and subiculum. By electron microscopy, the neurofibrillary tangles are composed of paired helical filaments ≈20 nm in diameter and with an axial periodicity of 80 nm. The second histopathological feature of the disease is the neuritic plaque (6–10). The fully developed neuritic plaque consists of an extracellular core of filaments 5–10 nm in diameter, which stain with Congo red, a characteristic shared by amyloid protein, cell debris, lipofuscin granules, and swollen degenerate neuritic processes filled with paired helical filaments, dense bodies, multilamellar bodies, and vesicles. This collection of degenerating neurites is frequently intertwined with glial processes.

In the present investigation, we report the use of fluorescence-activated cell sorting as an effective method for the final purification of the amyloid plaque core protein (APCP). The amino acid composition of the insoluble filaments of the APCP substantially differs from all forms of amyloids known. We also present details of their ultrastructural and chemical analyses.

MATERIALS AND METHODS

Source of Material. Human brains from patients who were clinically diagnosed as having Alzheimer disease were obtained within 4–12 hr postmortem. After removal of blood vessels and leptomeninges, adequate sections for histological diagnosis were taken from cortex and hippocampus and placed in formalin. The remaining hemispheres were frozen at −80°C until the time of biochemical processing. In every case, Alzheimer disease was confirmed by silver and thioflavin S staining before biochemical study. All experimental steps involved in the isolation of APCP were monitored by negative-stain electron microscopy using 1% uranyl acetate and by UV fluorescence microscopy following thioflavin S staining of the specimens.

Isolation of APCP. Approximately 500 g of neocortex, hippocampus, and amygdaloid nucleus were dissected from the underlying white substance, chopped finely, and suspended in 5 liters of 50 mM Tris·HCl, pH 7.4/2 mM EDTA/2% NaDodSO₄/1% 2-mercaptoethanol. After 16 hr of continuous stirring at room temperature, the suspension was sequentially filtered through a series of 210-, 152-, 86-, and 41-µm nylon meshes to eliminate large debris particles. The filtrate was centrifuged at 40,000 × g_{max} for 45 min, the supernatant was discarded, and the pellet was suspended in the buffer to a final vol of 1.2 liters, to which 120 g of solid sucrose was added, dissolved, and centrifuged at 1,500 × g_{max} for 1 hr. The resulting pellet was resuspended in 30% sucrose (wt/vol) prepared in the same buffer and centrifuged as described above. These pellets were then suspended in 30 ml of a 50% dilution of the original buffer, applied in aliquots of 5 ml to the top of a Ficoll-400 discontinuous density gradient [40%, 35%, 20%, 10% (wt/vol); 10 ml, 10 ml, 10 ml, and 5 ml, respectively] and centrifuged at 1500 × g_{max} for 1 hr. The 20–35% Ficoll interface was collected and washed four times with 50 mM Tris·HCl (pH 7.4). Removal of the small amounts of contaminating collagen was achieved by collagenase digestion (Worthington CLS III) at 37°C for 16 hr, under continuous stirring. To eliminate the enzyme and its proteolytic products, the specimen was washed and centrifuged five times (10,000 × g_{max}, 15 min) with distilled water. Staining with thioflavin S and negative-stain electron microscopy revealed an APCP-enriched specimen with lipofuscin contamination.

Fluorescent Labeling of APCP. The APCP was labeled with three fluorochromes: thioflavin S (11), thioflavin T (12), and

---

Abbreviations: APCP, amyloid plaque core protein; FACS, fluorescence-activated cell sorter.
†To whom reprint requests should be addressed: c/o Professor Robert Williamson, Department of Biochemistry, St. Mary's Hospital Medical School, Paddington, London, W2 1PG England.

phorwhite BBU (13). Fluorometric studies indicated that thioflavin S had a very close emission to the lipofuscin autofluorescence. Thioflavin T and phorwhite BBU, on the other hand, showed maximal excitation at 370 nm with an emission maximum of 418 nm for APCP and 450 nm for lipofuscin. We used the former fluorochrome because of the commercial unavailability of phorwhite BBU. The specimens were freshly labeled for 10 min with a 0.5% aqueous solution of thioflavin T containing 0.8% HCl. Unbound fluorochrome in the supernatant was removed by centrifugation (10,000 × g_{max}, 10 min). The resulting pellet was washed once with 1% acetic acid and three times with distilled water before resuspension in 50 mM Tris·HCl, pH 7.4/0.5% NaDodSO$_4$, and sonication at 25 kHz (10 W) for 60 sec.

Microfluorometric Purification. Final separation of APCP from lipofuscin was achieved with a Becton-Dickinson model 440 fluorescence-activated cell sorter (FACS) (14). The FACS was equipped with a 5-W argon laser beam tuned to a 60 mwatts multiple band UV spectrum (351–364 nm). The laser beam was further discriminated through a blocking filter (365 nm) and a long pass filter (400 nm). Fluorescent signals from the labeled APCP were detected by using a low range photomultiplier tube at 600 V, with a 420/20 nm band pass filter. Fluorescence data were recorded with a three decade logarithmic scale. The forward low angle scatter was detected with a light-sensitive diode having a 0.2 neutral density filter on a linear scale. All operations were carried out using a 70-μm nozzle tip vibrating at ≈30 kHz/sec. Sheath fluid (50 mM Tris·HCl, pH 7.4/0.5% NaDodSO$_4$) was pressurized at 14 psi (1 psi = 6.89 kPa). The sample pressure was adjusted to yield ≈4500 and 2000 total particle events per sec for the first and second passes, respectively. Sorting gates were set utilizing full-scale forward scattering against each of the two major fluorescent areas (those of APCP and lipofuscin). The deflection plates were positively and negatively charged at 2000 V each. Three fractions were collected: APCP, lipofuscin, and unseparated material. The percentages of particles sorted were calculated from single analysis displays

of fluorescence. The resulting data from the forward scattering and the logarithm of fluorescent information was collected and analyzed on a Becton Dickinson Consort 40 extended analysis system. The computer analysis consisted of single, bivariate, and three-dimensional displays, which were printed on a Hewlett–Packard 7476A graphics plotter.

Ultrastructure and Chemical Analysis. The FACS-purified material was negatively stained with 1% uranyl acetate on a Formvar-coated grid and observed with a JEOL 100 CX transmission electron microscope at 60 kV. Aliquots of the FACS-purified APCP and lipofuscin were pelleted and washed three times with distilled water (10,000 × g_{max}, 10 min) to remove unbound NaDodSO$_4$. The specimens were chemically modified by performic acid oxidation in 30 μl of formic acid (90% concentration) containing 3 μl of hydrogen peroxide (30% concentration) at 25°C for 1 hr. The reaction was terminated by the addition of 1.5 ml of distilled water and freeze drying. Approximately 100 μg of each specimen was submitted to acid hydrolysis (6 M HCl/1% phenol, 108°C), for 24, 48, and 72 hr. Amino acid analyses of APCP and lipofuscin were carried out on a Beckman 119 CL automatic analyzer with attached 126 data system.

After performic acid oxidation, APCP specimens were resuspended in 50 mM Tris·HCl, pH 7.5/0.2% NaDodSO$_4$, and negatively stained for electron microscopy. Aliquots were submitted to trypsin, chymotrypsin, pepsin, thermolysin, V8 protease, and proteinase K enzymic hydrolysis at an enzyme/substrate ratio of 1:25. Aliquots were also suspended in a variety of denaturing agents including 6 M guanidine hydrochloride, 6 M guanidine thiocyanate, and 8 M urea. Removal of tightly bound NaDodSO$_4$ was achieved by ion-pair extraction (15). One hundred micrograms of FACS-purified APCP was suspended in 300 μl of 90% formic acid, incubated at room temperature for 3 hr, and lyophilized. After removal of particulate material by centrifugation at 100,000 × g (Beckman airfuge) for 30 min, the specimens were submitted to high-performance liquid chromatography (Beckman 450-336-165 model) using a reversed-phase column
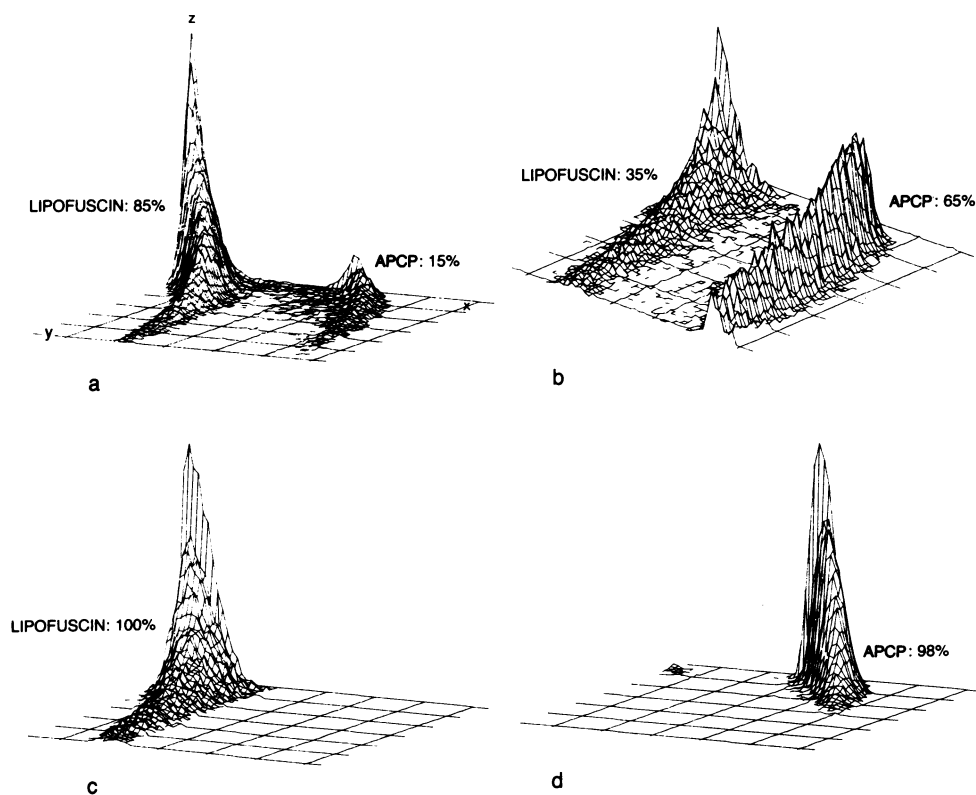

FIG. 1. Tridimensional histograms showing the progression of APCP and lipofuscin purification through the FACS. x, y, and z represent the forward light scattering, the blue log fluorescence, and the number of particle events analyzed, respectively. (*a*) Initial analysis of the sample prior to sorting. (*b*) Analysis after the first sorting pass of APCP and lipofuscin showing enrichment of the former from 15% to 65%; the specimen still contains 35% lipofuscin contamination. (*c* and *d*) Results of the second and final sorting pass. The lipofuscin and APCP were separated to 100% and 98% purity, respectively.

(Bio-Rad RP-318) with a gradient from 0% to 100% water/acetonitrile in 0.1% trifluoroacetic acid, and simultaneously monitored at 280 and 214 nm. NaDodSO$_4$/polyacrylamide gel electrophoresis at 10% and 20% concentration was carried out by the method of Laemmli (16).

RESULTS

Incorporation of EDTA in the initial NaDodSO$_4$/2-mercaptoethanol buffer resulted in a better liquefaction of the cerebral cortex, thus reducing the amount of insoluble material. Elimination of most of the contaminating membranous material, as well as a large quantity of lipofuscin and insoluble lighter neurofibrillary tangles, was achieved by the two sucrose (10% and 30%) extractions. The Ficoll-400 density-gradient centrifugation permitted the removal of a large quantity of basement membrane and other collagenous material derived from microvessels at the 0–10% interface and a large pellet of insoluble material resembling cell ghosts, perikarya, and amorphous debris at the bottom of the tube. The 20–35% interface contained a large quantity of APCP, lipofuscin granules, and some collagen fibers, which were eliminated by collagenase proteolysis.

As can be appreciated from Figs. 1 and 2, the purity of the APCP and secondarily of lipofuscin, on the basis of their fluorescent emission, approached 100%. The second sorting pass through the FACS, at 2000 total event particles per sec, yielded an average purification rate for APCP of 55% or 1100 particles per sec, with the rest of the particles being separated either as lipofuscin or as aborted events (microdroplets containing both lipofuscin and APCP). This latter material was recovered by centrifugation and resubmitted to FACS purification. From these data, we estimated the yield of purified APCP, from 1020 g of initial tissue (brains W-18 and W-19), to be $\approx 48 \times 10^6$. These two brains were particularly rich in amyloid plaques and showed, respectively, little and no evidence of cerebrovascular amyloid, at least in the histological sections examined. Allsop *et al.* (17) and Masters *et al.* (18), reported a yield of 2.5×10^4 and 5×10^5 cores per g of initial material, respectively, as compared to 4.8×10^4 obtained in our laboratory.

Electron microscopy of negatively stained FACS-purified APCP showed a homogeneous population of irregular dense masses, measuring between 2 and 14 μm, with frayed filamentous borders (Fig. 3a). Occasionally, the festooning filaments apparently detached from the large dense masses. These small filamentous conglomerates were very homogeneous, having 5.5- to 6.0-nm diameters and an indefinite length (Fig. 3b). The electron-dense cores appeared to consist of compacted random coils of filamentous structures. Treatment of APCP by performic acid oxidation dispersed the dense cores into a meshwork of filaments measuring an average of 10–12 nm in diameter and of variable length (Fig. 3 c and d). In contrast to paired helical filaments, which form the intracellular neurofibrillary tangles (19, 20), the core filaments appeared to have half their diameter and to be very flexible with fairly straight borders. The spreading of the neuritic plaque cores could be due to the strong interaction of concentrated formic acid with the hydrogen bonds, acting as a proton donor to the carbonyl of the amide groups and to the perturbance of hydrophobic interactions between nonpolar residues. Furthermore, the action of hydrogen peroxide on cysteine yielding cysteic acid may have played an additional role in their dispersion. Resuspension in 0.2% NaDodSO$_4$ followed by sonication broke the long filaments into smaller random pieces, which did not pellet at $100,000 \times g$. Reversed-phase HPLC of the NaDodSO$_4$ stripped filaments, which had been previously incubated in concentrated formic acid, produced a broad peak eluted between 55% and 100% acetonitrile concentration, resulting from randomly sized

filamentous structures. Acrylamide gel electrophoresis also failed to produce discrete banding from chemically or enzymatically treated filaments. Other investigations (17, 18) have also found APCP to be insoluble in a variety of protein denaturants and detergents, a characteristic shared by Alzheimer paired-helical filaments (21). However, Masters *et al.* (18) apparently succeeded in partially solubilizing the amyloid plaque cores after treatment with 90% formic acid. In our experience, once the concentrated formic acid is removed, a step necessary for further characterization, the amyloid plaque cores dispersed into an array of discrete filaments (see Fig. 3c) and, depending on concentration, also failed to pellet at high-speed centrifugation.

As in the case of APCP, the grossly insoluble lipofuscin, which forms a turbid suspension of yellow-brown autofluorescent neuronal granules (1- to 3-μm diameter), was rendered optically clear by the performic acid modification. This may have been due to oxidation of polyunsaturated lipids into ethylenic peroxides and to the oxidation of cysteine and methionine into cysteic acid and methionine sulfone, having the double solubilizing effect of increasing hydration and electrostatic repulsion.
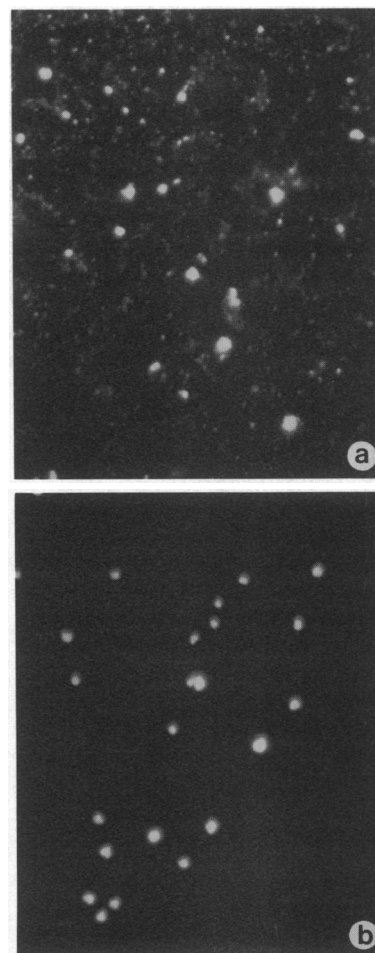

FIG. 2. Fluorescence microscopy photographs of thioflavin T-labeled APCP. (a) Prior to FACS purification. The large bright fluorescent particles represented APCP. The smaller and duller granular background is the autofluorescent contaminating lipofuscin. This photograph corresponds to stage a of Fig. 1. (b) After two sorting passes through FACS, the APCP is purified to 98%. This photograph corresponds to stage d of Fig. 1. The size of the sorted neuritic plaque cores ranged from 2 to 14 μm. Photographs were taken with a Zeiss UV microscope with an excitation filter G-365 and a barrier filter LP-420. ($\times$290.)
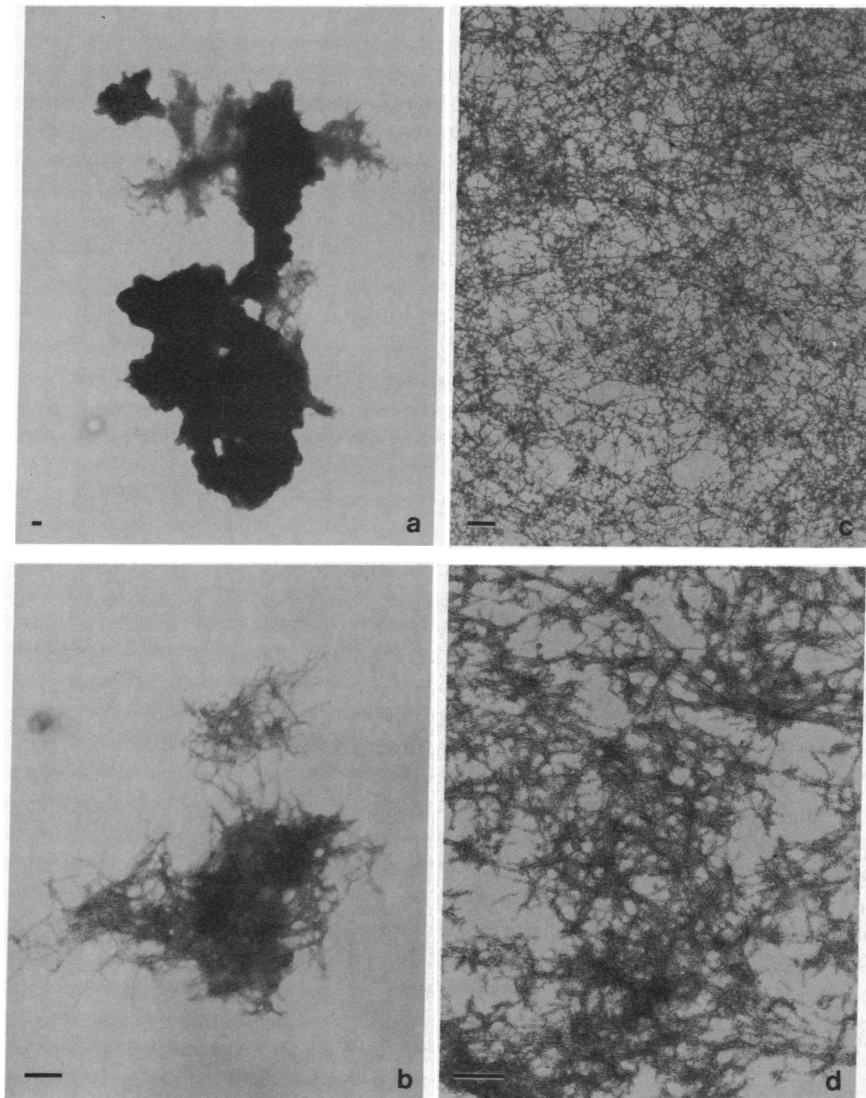
FIG. 3. Electron micrographs of FACS-purified APCP. (*a*) Micrograph showing a dense amyloid plaque core with festooning filaments 5.5–6.0 nm in diameter. (×12,800.) (Bar = 0.1 μm.) (*b*) Micrograph of a small aggregate of festooning filaments 5.5–6.0 nm in diameter detached by sonication. (×48,400.) (Bar = 0.1 μm.) (*c*) Micrograph of the APCP after performic acid oxidation. The dense amyloid plaque cores shown in *a* were dispersed into an array of 10–12 nm diameter filaments of variable length. (×3750.) (Bar = 1 μm.) (*d*) Same filaments as in *c*. (×67,300.) (Bar = 0.1 μm.)

The total amino acid compositions of APCP and of lipofuscin (Table 1) were very different, suggesting a minimum amount of cross-contamination between the FACS-derived fractions. The amino acid analysis of APCP showed a high content of hydrophobic residues. Glycine and valine alone accounted for 30% of the molecule(s). Furthermore, no derivatives of proline, histidine, tyrosine, or lysine were found, as there were no additional chromatographic peaks to those corresponding to the common amino acids. The overall composition of the molecule indicates an acidic isoelectric point. The total amino acid compositions of the APCP determined by workers in other laboratories differed from that presented here, although there is an overall resemblance highlighted by the predominance of hydrophobic residues. The compositions obtained by Allsop *et al.* (17) are the closest to our own results, those from Masters *et al.* (18) differ more, and those from Glenner and Wong (22) differ most. However, we should acknowledge that the latter investigation dealt with the cerebrovascular amyloid protein obtained from individuals with Alzheimer disease with congophilic angiopathy. Nevertheless, the differences among the groups could be the result of different purification protocols or different degrees of contamination or individual heterogeneity.

The amino acid composition of the APCP was submitted to the protein and nucleic acid sequence databases at the National Biomedical Research Foundation (Washington, DC). The computerized search indicated that APCP did not resemble any proteins so far known. Significantly, the composition differed substantially from those of actin, tubulin, neurofilament triplet proteins, glial acidic fibrillary protein, vimentin, desmin, keratins, amyloid proteins found in the inherited systemic and localized amyloidoses, and the scrapie "prions."

DISCUSSION

We have found like others (10, 17, 18) that density-gradient centrifugation is an excellent technique for the enrichment of APCP of Alzheimer disease. However, this technique has the disadvantage of carrying a variable amount of contamination. Because of this limitation, we developed a technique that uses microfluorometric sorting for the final purification step of APCP. This was based on (*i*) the insolubility and dimensions of the highly aggregated state of APCP and (*ii*) the ability of this protein for uptaking the fluorochrome thioflavin T in the presence of NaDodSO$_4$, which maintains the protein cores separated from each other as well as from lipofuscin granules, its main contaminant.

The purified APCP is composed of amorphous compact aggregates, which most probably correspond to the centrally situated masses in the so-called "classic" and "burned out" plaques (23), irregularly decorated by festooning aggregates of 5.5- to 6.0-nm diameter filaments. After performic acid oxidation, the APCP is dispersed into an array of discrete 10- to 12-nm diameter filaments. Our preliminary studies on the

Table 1. Amino acid composition of APCP and lipofuscin

	APCP, mol per 100 residues*	Lipofuscin, mol per 100 residues*
Cys†	1.0	16.3
Asp	7.9	8.2
Met†	2.6	1.5
Thr‡	1.6	4.1
Ser‡	4.9	6.4
Glu	9.8	7.8
Pro	0.9	2.7
Gly	15.8	12.5
Ala	8.7	6.3
Val§	14.2	8.1
Ile§	6.3	4.3
Leu	6.1	7.7
Tyr	1.9	2.3
Phe	6.0	5.1
His	5.3	0.9
Lys	5.1	3.3
Arg	1.9	2.5
Trp	ND	ND

ND, not determined.

*Average values from determinations at 24, 48, and 72 hr hydrolysis (6 M HCl, 108°C) except as noted.

†Quantitated as cysteic acid and methionine sulfone following performic acid oxidation.

‡Extrapolated to 0-hr hydrolysis value.

§72-hr hydrolysis value.

latter filaments suggest a bifilar helical structure as described (24, 25). It is possible that the festooning 5.5- to 6.0-nm filaments could represent a precursor form of the 10- to 12-nm filaments, or, conversely, a product of its dissociation by the action of enzymes at the surface of the amyloid plaque core, or they could be different.

The total amino acid composition of the FACS-purified APCP seems to indicate either a large protein(s) or a heterogeneous mixture of medium sized ones, rather than a 4-kDa monomeric subunit, as recently published (18). In this respect, we encountered difficulties in accommodating the deviations and heterogeneity of the total amino acid compositions, from our laboratory and others (17, 18), into a polypeptide with a theoretical length of 36–40 amino acids, when one considers that the sequence of the first 28 amino acids is known (18).

It is fairly well accepted that Alzheimer disease differs only quantitatively from the normal aging process of the brain. Thus, as better public health control of the major killing diseases occurs, the opportunity for development of such age-related processes will increase (26). Paralleling this will undoubtedly be the accumulation of other neuronal inclusions such as lipofuscin. The population of lipofuscin concentrated at the 20% to 35% Ficoll interface contains 16 mol % cysteine, thereby grouping this protein with the high sulfur-containing proteins like some of the keratins, enzyme inhibitors, growth factors (27–29), and metallothioneins (30). The latter family of proteins specifically bind heavy metals (zinc, cadmium, copper, mercury, etc.) and are involved in detoxification and cellular homeostasis. In this respect, it is worth mentioning that lipofuscin has been found to contain significant quantities of divalent cations (e.g., copper, manganese, calcium, iron, zinc) (31), which are most probably bound in the form of mercaptides. In light of recent reports associating neurofibrillary tangles with calcium and magne-

sium deficiencies in some human encephalopathies (32), one may suspect some role of lipofuscin in Alzheimer disease.

If the filaments of Alzheimer disease are intrinsic to the central nervous system, it would be of prime importance to investigate the regulatory genetic mechanisms that promote their synthesis and accumulation and, ultimately, the pathologic transformation of the cell and extracellular space. It is hoped that the purification of the APCP and lipofuscin reported here will advance our understanding of aging phenomena in general and of Alzheimer disease in particular.

1. Terry, R. D. & Katzman, R. (1983) *Ann. Neurol.* **14**, 497–506.
2. Tomlinson, B. E. & Corsellis, J. A. N. (1984) in *Greenfields' Neuropathology*, eds. Hume-Adams, J., Corsellis, J. A. N. & Duchen, L. W. (Wiley, New York), pp. 951–1025.
3. Wells, C. E. (1985) in *Comprehensive Textbook of Psychiatry*, eds. Kaplan, H. I. & Sadock, B. J. (Williams & Wilkins, Baltimore), pp. 851–869.
4. Mortimer, J. A., Schuman, L. M. & French, L. R. (1981) in *The Epidemiology of Dementia*, ed. Mortimer, J. A. & Schuman, L. M. (Oxford Univ. Press, New York), pp. 3–23.
5. Terry, R. D. (1963) *J. Neuropathol. Exp. Neurol.* **22**, 629–642.
6. Kidd, M. (1964) *Brain* **87**, 307–327.
7. Terry, R. D., Gonatas, N. K. & Weiss, M. (1964) *Am. J. Pathol.* **44**, 269–297.
8. Luse, S. A. & Smith, K. R. (1964) *Am. J. Pathol.* **44**, 553–563.
9. Krigman, M. R., Feldman, R. G. & Bensch, K. (1965) *Lab. Invest.* **14**, 381–396.
10. Nikaido, T., Austin, J., Rinehart, R., Trueb, L., Hutchinson, J., Stukenbrok, H. & Miles, B. (1971) *Arch. Neurol.* **25**, 198–211.
11. Kelenyi, G. (1967) *J. Histochem. Cytochem.* **15**, 172–180.
12. Burns, J., Pennock, C. A. & Stoward, P. J. (1967) *J. Pathol. Bacteriol.* **94**, 337–344.
13. Waldrop, F. S., Puchtler, H. & Valentine, L. S. (1973) *Arch. Pathol.* **95**, 37–41.
14. Herzenberg, L. A., Sweet, R. G. & Herzenberg, L. A. (1976) *Sci. Am.* **234**, 108–117.
15. Konigsberg, W. H. & Henderson, L. (1983) *Methods Enzymol.* **91**, 254–259.
16. Laemmli, U. K. (1970) *Nature (London)* **227**, 680–685.
17. Allsop, D., Landon, M. & Kidd, M. (1983) *Brain Res.* **259**, 348–352.
18. Masters, C. L., Simms, G., Weinman, N. A., Multhaup, G., McDonald, B. L. & Beyreuther, K. (1985) *Proc. Natl. Acad. Sci. USA* **82**, 4545–4549.
19. Wisniewski, H. M., Merz, P. A. & Iqbal, K. (1984) *J. Neuropathol. Exp. Neurol.* **43**, 643–656.
20. Wischik, C. M., Crowther, R. A., Steward, M. & Roth, M. (1985) *J. Cell Biol.* **100**, 1905–1912.
21. Selkoe, D. J., Ihara, Y. & Salazar, F. J. (1982) *Science* **215**, 1243–1245.
22. Glenner, G. C. & Wong, W. C. (1984) *Biochem. Biophys. Res. Commun.* **120**, 885–890.
23. Terry, R. D. & Wisniewski, H. M. (1972) *Adv. Behav. Biol.* **3**, 89–116.
24. Narang, H. K. (1980) *J. Neuropathol. Exp. Neurol.* **39**, 621–631.
25. Merz, P. A., Wisniewski, H. M., Sommerville, R. A., Bobin, S. A., Masters, C. L. & Iqbal, K. (1983) *Acta Neuropathol.* **60**, 113–124.
26. Cutler, R. G. (1984) in *Aging and Cell Function*, ed. Johnson, J., Jr. (Plenum, New York), pp. 1–147.
27. Hunt, L. T. & Dayhoff, M. O. (1976) in *Atlas of Protein Sequence and Structure*, ed. Dayhoff, M. O. (Nat'l. Biomed. Res. Found., Washington, DC), Suppl. 2, pp. 233–244.
28. Barker, W. C. & Dayhoff, M. O. (1976) in *Atlas of Protein Sequence and Structure*, ed. Dayhoff, M. O. (Nat'l. Biomed. Res. Found., Washington, DC), Suppl. 2, pp. 105–112.
29. Hunt, L. T. & Dayhoff, M. O. (1978) in *Atlas of Protein Sequence and Structure*, ed. Dayhoff, M. O. (Nat'l. Biomed. Res. Found., Washington, DC), Suppl. 3, pp. 265–272.
30. Karin, M. & Richards, R. J. (1982) *Nature (London)* **299**, 797–802.
31. Siakotos, A. N. & Armstrong, D. (1975) in *Neurobiology of Aging*, eds. Ordy, J. M. & Brezzee, K. R. (Plenum, New York), pp. 369–399.
32. Gajdusek, D. C. (1985) *N. Engl. J. Med.* **312**, 714–719.